Isotope thermometry in nuclear multifragmentation

B. K. Agrawal and S. K. Samaddar
Saha Institute of Nuclear Physics, 1/AF Bidhannagar, Calcutta 700 064, India

Tapas Sil and J. N. De
Variable Energy Cyclotron Centre, 1/AF Bidhannagar, Calcutta 700 064, India
(Received 25 September 1998)

A systematic study of the effect of fragment-fragment interaction, quantum statistics, γ-feeding, and collective flow is made in the extraction of the nuclear temperature from the double ratio of the isotopic yields in the statistical model of one-step (prompt) multifragmentation. Temperature is also extracted from the isotope yield ratios generated in the sequential binary-decay model. Comparison of the thermodynamic temperature with the extracted temperatures for different isotope ratios show some anomaly in both models which is discussed in the context of experimentally measured caloric curves. [S0556-2813(99)06002-1]

PACS number(s): 25.70.Pq, 24.10.Pa

I. INTRODUCTION

The response of nuclei to high excitations or temperatures has been a subject of intense study both theoretically and experimentally for the last several years. From theoretical investigations of hot nuclear matter [1–3] and also of finite nuclei [4], it has been suggested that the nuclear system may undergo a liquid-gas phase transition at high temperatures. Recent experimental measurements of the nuclear caloric curve by the ALADIN Group [5] in the Au+Au collisions at 600*A* MeV tentatively support such a conjecture. The key element that enters in such a surmise is the extraction of the nuclear temperature that they observed to be nearly constant in the excitation energy range of $\sim 3-10$ MeV per nucleon beyond which the caloric curve rises almost linearly with a slope close to that of a classical gas. Experimental data from the EOS Collaboration [6,7] are also suggestive of critical behavior in nuclei; here too exact determination of the nuclear temperature has the most essential role to play.

The temperatures of hot fragmenting systems are generally measured from the double ratios of isotope multiplicities employing the prescription proposed by Albergo *et al.* [8] based on the statistical model of prompt multifragmentation (PM) [9]. In arriving at the prescription, several simplifying assumptions are made, namely, (i) the fragments are noninteracting, (ii) the fragments follow Maxwell-Boltzmann distribution, (iii) they are formed in their ground states and (iv) all their kinetic energies are in the thermal mode, i.e., collective flow energy is absent. The effects of the interaction have later been simulated through an effective excluded volume interaction [10]; to our knowledge, the effect of fragment-fragment interaction on the isotope ratio temperature (T_r) within the freeze-out configuration has however not been taken into account. Though it is expected that at high temperatures and low densities the quantum system would behave like a classical Maxwell-Boltzmann system, the importance of invoking quantum statistics in multifragmentation has been emphasized by several authors [10–12]. The qualitative effect of quantum statistics is to increase the number of bosons with respect to fermions at low temperatures and high densities, the isotope ratio and hence the extracted temperature T_r might have some sensitivity to the choice of statistics. The assumption of the formation of the fragments in their ground states is an oversimplification. In general, the fragments are expected to be formed in various excited states which are not too short-lived. These excited fragments subsequently decay either by particle or γ-ray emission. These side-feeding effects are shown [10,13–15] to have an important bearing on the observed multiplicities and hence on the deduced nuclear temperature. The hot fragmenting nuclear complex that is formed in nuclear collisions may be compressed depending on the collision geometry which subsequently decompresses to the freeze-out configuration generating significant amount of collective nuclear flow energy. The important role played by collective flow on the fragmentation pattern has been shown earlier [16,17]. Its effect on the nuclear temperature has only been qualitatively studied by Shlomo *et al.* [18] and found to be nonnegligible. In a systematic step by step approach, we explore in this paper the effects of the four approximations listed earlier on the isotopic temperatures by considering different isotope double ratios and examine whether they can be considered as good pointers to the thermodynamic temperature of the fragmenting system.

The physics of the nuclear multifragmentation is not yet fully established beyond question. The one-step prompt break-up (PM) looks a very plausible scenario at high excitations and the sequential binary decay (SBD) model [19,20] may provide a better description of the reaction mechanism at lower excitation. Both these processes are thermal in nature. From the inclusive mass or charge distributions or even the scaling of the multiplicities of the intermediate mass fragments (IMF), it is however difficult [21] to discuss the relative merits of these two competing models. If the SBD model is the more viable model, say, for the yield of nuclear fragments in nuclear collisions, then the Albergo prescription of extracting nuclear temperature from the double isotope ratios is called into question. One notes that in the SBD model, there is no unique temperature but a succession of temperatures till the nuclear fragments are produced in their particle stable configurations. It would still be interesting to know what values of temperatures one extracts from double

ratios in the SBD model and whether they can offer some added insight in the nature of nuclear disassembly.

The paper is organized as follows. In Sec. II, we briefly outline the PM and SBD models. In Sec. III, temperatures calculated from both models are presented and discussed in the context of experimental data. The conclusions are drawn in Sec. IV.

II. THEORETICAL FRAMEWORK

The multiplicities of fragments produced in nuclear collisions are experimentally measured quantities; the nuclear temperature is a derived entity. In the following, we outline the models for fragment production and relate the nuclear temperature to the fragment yield.

A. Prompt multifragmentation

A hot nuclear system with N_0 neutrons and Z_0 protons may be formed in nuclear collisions at a temperature T_0 with excitation energy ϵ^* per particle. It may be initially compressed in a volume smaller than its normal volume. The compressed matter decompresses and develops a collective radial flow in addition to thermal excitation. We still assume that the system evolves in thermodynamic equilibrium and undergoes multifragmentation after reaching the ''freeze-out'' volume at a temperature T different from T_0. If the time scale involved in expansion is larger compared to the equilibration time in the expanding complex (i.e., the expansion is quasistatic), this assumption is not unjustified . We further assume that at the freeze-out volume, the system reaches chemical equilibrium.

The expansion of the compressed system may be simulated through a negative external pressure [16]. If there was no flow, at the freeze-out, the kinetic contribution of the thermal pressure is generally assumed to be cancelled by interaction contributions, i.e., the system is at equilibrium under zero external pressure. A positive pressure corresponds to compression of the system; similarly a negative pressure would cause decompression. If P_i is the internal partial pressure exerted by the radially outflowing fragments of the ith species at the surface, the total external pressure P is then given by $P=-\Sigma_i P_i$. The total thermodynamic potential of the system at the freeze-out volume is given by [16,22]

$$G=E-TS-\sum_{i=1}^{N_s}\mu_i\omega_i+P\Omega, \tag{1}$$

where E and S are the internal energy and entropy of the system, $\Omega=V-V_0$ with V as the freeze-out volume and V_0 the normal nuclear volume of the fragmenting system, N_s the total number of fragment species, μ_i the chemical potential and ω_i the multiplicity. The occupancy of the fragments is obtained by minimizing the total thermodynamic potential G and is given by

$$n_i(p_i)=\frac{1}{\exp\{(e_i-\mu_i)/T\}\pm 1}, \tag{2}$$

where $(\pm)$ sign refers to the fermionic and bosonic nature of the fragments. The single particle energy e_i is [16,23]

$$e_i=\frac{p_i^2}{2m_i}-B_i+\mathcal{V}_i-\frac{P_i}{\rho_i}. \tag{3}$$

Here B_i refers to the binding energy, ρ_i is the density of the ith fragment species obtained from the momentum integration of the distribution function given by Eq. (2) and $\mathcal{V}_i$ corresponds to the single particle potential, evaluated in the complementary fragment approximation [24,25]. It is given by

$$\mathcal{V}_i=\frac{\int \exp[-U_i(R)/T]U_i(R)d^3R}{\int \exp[-U_i(R)/T]d^3R}, \tag{4}$$

where $U_i(R)$ is the interaction energy of the fragment with its complementary at a separation R and the integration is over the whole freeze-out volume with the exclusion of the volume of the complementary fragment. Under chemical equilibrium, the chemical potential of the ith fragment species is

$$\mu_i=\mu_n N_i+\mu_p Z_i. \tag{5}$$

The neutron and proton chemical potentials μ_n and μ_p are obtained from the conservation of baryon and charge number, N_i and Z_i being the number of neutrons and protons in the fragment . The fragment yield is obtained from the phase-space integration of the occupancy function and for fermions it is given by

$$\omega_i=\frac{2}{\sqrt{\pi}}\Omega\lambda_i^{-3}J_{1/2}^{(+)}(\eta_i)\phi_i(T). \tag{6}$$

For bosons, the corresponding multiplicity is given by

$$\omega_i=g_0[e^{-\eta_i}-1]^{-1}+\frac{2}{\sqrt{\pi}}\Omega\lambda_i^{-3}J_{1/2}^{(-)}(\eta_i)\phi_i(T). \tag{7}$$

In Eqs. (6) and (7), η_i is the fugacity defined as

$$\eta_i=\frac{\mu_i+B_i-\mathcal{V}_i+P_i/\rho_i}{T}, \tag{8}$$

$\lambda_i=h/\sqrt{2\pi m_i T}$ is the thermal wavelength with m_i as the mass of the ith fragment species and $J_{1/2}^{(\pm)}$ are the Fermi and Bose integrals [26] given by

$$J_{1/2}^{(\pm)}(\eta)=\int_0^\infty \frac{x^{1/2}dx}{\exp\{(x-\eta)\}\pm 1}. \tag{9}$$

The first term on the right-hand side of Eq. (7) gives the number of condensed bosons, g_0 being their ground state spin degeneracy. The quanity $\phi_i(T)$ is the internal partition function of the fragments and is defined as

$$\phi_i(T)=\sum_s g_s e^{-\epsilon_s^*(i)/T}, \tag{10}$$

where g_s is the spin degeneracy of the excited state s of the cluster with excitation energy $\epsilon_s^*(i)$. The flow pressure P_i is shown to be related [16] to the flow energy E_i of the ith species in the form

$$\frac{P_i}{\rho_i} = C(v_{fi}, T) E_i, \tag{11}$$

where C is dependent on the fragment species, the temperature and also on the flow velocity of the fragments v_{fi}. It is found to be close to 4 except for very light fragments.

In the limit $\eta_i \ll 0$ (which is true when the density is very low), $J_{1/2}^{(+)}(\eta) \rightarrow (\sqrt{\pi}/2) e^{\eta}$, and then from Eq. (6) the yield of the fermion fragments reduces to

$$\omega_i = \Omega \lambda_T^{-3} A_i^{3/2} e^{\eta} \phi_i(T), \tag{12}$$

where $\lambda_T = h/\sqrt{2\pi m T}$ is the nucleon thermal wavelength with m as the nucleon mass and A_i the mass number of the ith fragment species. In the same limit, Eq. (7) for boson yield reduces also to Eq. (12). This is also the result obtained from the classical Maxwell-Boltzmann distribution.

If one chooses two sets of fragment pairs $(A_1, Z_1), (A_1', Z_1')$ and $(A_2, Z_2), (A_2', Z_2')$ such that $Z_1' = Z_1 + p$, $Z_2' = Z_2 + p$, $N_1' = N_1 + n$, $N_2' = N_2 + n$ where n and p are integers, then from Eq. (12) it follows that the measured double ratio R_2 of the fragment yields can be used to determine the temperature of the fragmenting system:

$$R_2 = \frac{\omega(A_1', Z_1')/\omega(A_1, Z_1)}{\omega(A_2', Z_2')/\omega(A_2, Z_2)} = \left(\frac{A_1' A_2}{A_1 A_2'}\right)^{3/2} \times \frac{\phi(A_1', Z_1', T)\, \phi(A_2, Z_2, T)}{\phi(A_1, Z_1, T)\, \phi(A_2', Z_2', T)} e^{(\Delta B/T)} e^{-(\Delta \mathcal{V}/T)} e^{(\Delta F/T)}, \tag{13}$$

where

$$\Delta B = B(A_1', Z_1') - B(A_1, Z_1) + B(A_2, Z_2) - B(A_2', Z_2'),$$
$$\Delta \mathcal{V} = \mathcal{V}(A_1', Z_1') - \mathcal{V}(A_1, Z_1) + \mathcal{V}(A_2, Z_2) - \mathcal{V}(A_2', Z_2'),$$
$$\Delta F = C[E(A_1', Z_1') - E(A_1, Z_1) + E(A_2, Z_2) - E(A_2', Z_2')]. \tag{14}$$

In the limit of low density, the nuclear part of the single-particle potential becomes relatively unimportant; further choosing $p = 0$ and $n = 1$, the Coulomb contribution to $\Delta \mathcal{V}$ practically vanishes.

Albergo *et al.* [8] further assumed the fragments to be formed in their ground states and they did not consider any collective flow. Then with $\Delta F = 0$ and $\Delta \mathcal{V} = 0$ the temperature is easily determined from

$$R_2 = \left(\frac{A_1' A_2}{A_1 A_2'}\right)^{3/2} \frac{g_0(A_1', Z_1', T) g_0(A_2, Z_2, T)}{g_0(A_1, Z_1, T) g_0(A_2', Z_2', T)} e^{(\Delta B/T)} \tag{15}$$

since the ground state degeneracy $g_0(A,Z)$ and binding energies are *a priori* known.

If prompt multifragmentation is the real physical mechanism for fragment production, Eq. (15) then provides an approximate but simple way to find out the thermodynamic temperature of the disassembling system. Influences from other effects as already mentioned are however embedded in the experimental data for isotope yield ratios. One cannot obtain informations on the perturbations caused by these effects on the double-ratio thermometer simply from the experimental isotopic yields without the help of further model calculations. If there were no other effects except from side-feeding through γ-decay, the experimental data could be exploited to delineate side-feeding effects by using Eq. (13) with $\Delta \mathcal{V} = 0$ and $\Delta F = 0$ with the choice of the internal partition function from Eq. (10). Effects from particle decay [13] or those coming from the inclusion of Coulomb force for yield ratios involving isotopes differing by proton number [27] could also be approximately reconstructed from the experimental fragment multiplicities. Influence of nuclear interaction, quantum statistics or collective expansion cannot however be singled out without recourse to models. We have therefore done calculations in the prompt multifragmentation model with the barest scenario (classical statistics, no interaction, no side-feeding, and no nuclear flow) and then included the said effects step by step to generate fragment multiplicities. The multiplicities so generated under different approximations are used to extract double-ratio temperatures using Eq. (15) to delineate the role of various effects on the temperatures.

B. Sequential binary decay

Fragmentation may also proceed via a sequence of binary fissionlike events, particulary at relatively lower excitation energies. We employ the transition-state model of Swiatecki [19] to find the decay probability of a hot nucleus with mass A, charge Z and excitation energy E^* into two fragments of mass and charge (A_1, Z_1) and $(A - A_1, Z - Z_1)$, respectively. At the saddle point, the binary fragmentation probability is given by

$$P(A, Z, E^*; A_1, Z_1) \propto \exp[2\sqrt{a(E^* - V_B - K)} - 2\sqrt{aE^*}], \tag{16}$$

where a is the level density parameter taken as $A/10$ MeV^{-1}, K is the relative kinetic energy at the saddle point, and V_B the barrier height dependent on the saddle point temperature T_s which is different from the temperature T_0 of the parent nucleus given by $T_0 = \sqrt{E^*/a}$. The barrier height is determined in the two sphere approximation as

$$V_B(T_s) = V_c + V_N + E_{\rm sep}(T_0, T_s), \tag{17}$$

where $E_{\rm sep}$ is the separation energy. It is evaluated as

$$E_{\rm sep}(T_0, T_s) = B(T_0) - B_1(T_s) - B_2(T_s). \tag{18}$$

The binding energies are taken to be temperature dependent [25]. The saddle-point temperature which is also the temperature of the fragmented daughter nuclei is given as

$$T_s = \sqrt{(E^* - V_B - K)/a}. \tag{19}$$

The evaluation of T_s from Eq. (19) requires a knowledge of the relative kinetic energy K. We assume it to follow a thermal distribution $P(K) \propto \sqrt{K} e^{-K/T_s}$. The complicated interrelationship between V_B, K and T_s renders evaluation of T_s difficult; to simplify the problem, K in Eq. (19) is replaced by its average value $\frac{3}{2}T_s$ and then T_s is evaluated in an iterative procedure with T_0 as the starting value. This is expected to be a good approximation since the dispersion in kinetic energy is of the $\sim T_s$ and (E^*-V_B) is generally much greater than T_s. The so extracted value of T_s is used only to evaluate the barrier V_B from Eq. (17), the decay probability and the thermal distribuion. In Eq. (17), V_c is the Coulomb interaction taken to be that between two uniformly charged spheres and V_N is the interfragment nuclear interaction [25].

The relative kinetic energy K of the two fragmented nuclei lying in the range $0 \leqslant K \leqslant (E^*-V_B)$ is generated in a Monte Carlo method obeying the thermal distribution as mentioned. To ensure energy conservation, this kinetic energy is plugged into Eq. (19) to evaluate the temperature of the daughter nuclei for further dynamical evolution. The fragment kinetic energy and hence their velocities are obtained from momentum conservation.

The trajectories of the fragments are calculated under the influence of Coulomb interaction in the overall center of mass frame. If the fragments have sufficient excitation energy, they decay in flight. The integration of the trajectories is continued till the asymptotic region is reached when the interaction energy is very small (~ 1 MeV) and the excitation energy of the fragments are below particle emission threshold.

III. RESULTS AND DISCUSSIONS

In this section we present the results of the calculations for temperatures extracted from double ratios of different isotope yields obtained from nuclear multifragmentation. These calculations are performed under different approximations mentioned in the introduction in the PM model. For this purpose we have taken ^{150}Sm as a representative case for the fragmenting system. We also obtained the double ratio temperatures assuming that the fragmentation proceeds via sequential binary decay.

A. Prompt multifragmentation

The initial temperature T_0 of the hot system formed is different from the kinetic temperature T (also referred to as the thermodynamic temperature) of the fragments at the freeze-out. What remains constant is the total energy E of the system or equivalently its excitation energy $E^*=E+B_0$ where B_0 is the binding energy of the system. The total energy of the fragmented system may be written as

$$E=\frac{3}{2}T(M-1)-\sum_{i=1}^{N_s}\omega_i B_i+\frac{1}{2}\sum\omega_i\mathcal{V}_i+\sum\omega_i\langle\epsilon^*(i)\rangle, \tag{20}$$

where $M=\Sigma_i\omega_i$ is the total number of the fragments produced in the grand canonical model for PM and $\mathcal{V}_i$ the single-particle potential. The quantity $\langle\epsilon^*(i)\rangle$ is the average excitation energy of the ith fragment species given by

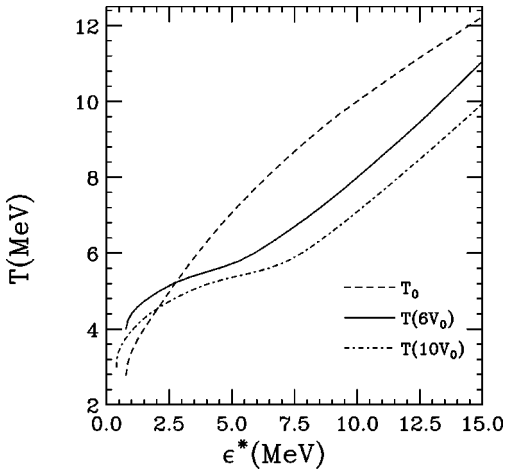

FIG. 1. The temperature of the fragmenting system ^{150}Sm as a function of ϵ^*, the excitation energy per nucleon. The dashed line (T_0) corresponds to the temperature in the Fermi-gas approximation; the full and dot-dash lines refer to temperatures at the freeze-out volumes taken to be $6V_0$ and $10V_0$, respectively.

$$\langle\epsilon^*(i)\rangle=\frac{\int\epsilon\rho_i(\epsilon)e^{-\epsilon/T}d\epsilon}{\int\rho_i(\epsilon)e^{-\epsilon/T}d\epsilon}, \tag{21}$$

where the integrations extend up to the particle emission threshold and ρ_i is the level density obtained from Bethe ansatz [20]. To compare the temperature T and T_0 taken as $T_0=\sqrt{E^*/a}$, we plot in Fig. 1 these temperatures as a function of $\epsilon^*=E^*/A$, the excitation energy per particle. The dashed line corresponds to the temperature T_0 and the solid and dot-dash lines correspond to the thermodynamic temperatures evaluated at the freeze-out volumes $6V_0$ and $10V_0$ respectively, V_0 being the normal volume of the fragmenting system. The curve for T_0 is parabolic but it is interesting to note that the caloric curves corresponding to the different freeze-out volumes mentioned show plateaux in the excitation energy. In the canonical model of multifragmentation with multiplicity-dependent freeze-out volume, Bondorf *et al.* [4] reported first such a plateau reminiscent of the onset of a phase transition in nuclei. With increase in freeze-out volume, we find in our calculation that the temperature decreases and the plateau gets extended in the excitation energy. Such a dependence of caloric curve on the freeze-out volume was also observed in a self-consistent Thomas-Fermi calculation [28].

In Figs. 2–7, we display the isotope double ratio temperatures T_r from the prompt breakup of ^{150}Sm with different choices of isotope combinations fixing the freeze-out volume at $6V_0$. The combinations are (^{4}He/^{3}He)/(d/p), (^{4}He/^{3}He)/(t/d), (^{7}Li/^{6}Li)/(d/p), (^{7}Li/^{6}Li)/(^{4}He/^{3}He), (^{10}Be/^{9}Be)/(^{4}He/^{3}He), and (^{13}C/^{12}C)/(^{7}Li/^{6}Li). They would be referred to as (He-d), (He-t), (Li-d), (Li-He), (Be-He), and (C-Li), respectively. In all these figures, the dotted lines correspond to the temperatures obtained from the multiplicities generated in the barest Albergo prescription

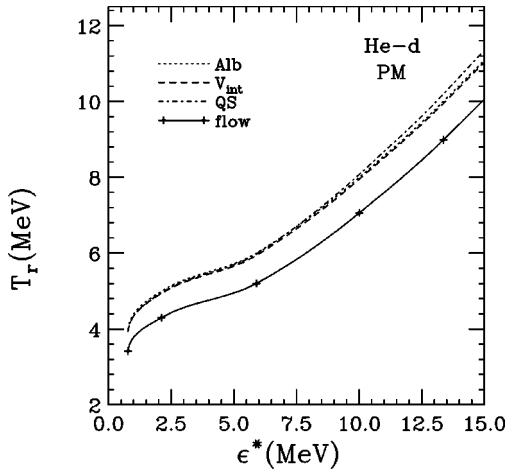

FIG. 2. The temperature T_r from the double-ratio $(^4\mathrm{He}/^3\mathrm{He})/(d/p)$ for the system ^{150}Sm as a function of ϵ^* in the prompt multifragmentation model. The dotted line refers to T_r obtained from Albergo prescription; the dashed, dot-dash, and full line with crosses correspond to the temperatures with subsequent progressive inclusion of final state interaction, quantum statistics, and flow energy, taken to be one-fourth of the total excitation.

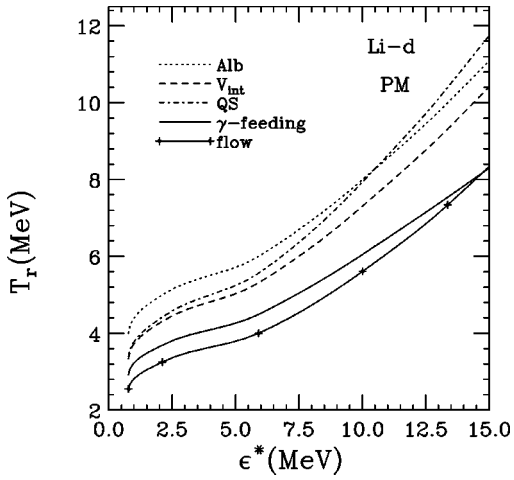

FIG. 4. The temperature T_r from the yield ratio $(^7\mathrm{Li}/^6\mathrm{Li})/(d/p)$ in the PM model. The dotted line refers to the Albergo prescription; the dashed, dot-dash, full line, and line with crosses refer to T_r with subsequent step by step inclusion of final state interaction, quantum statistics, γ-feeding, and flow energy, taken to be one-fourth of the total excitation.

as mentioned earlier. It is obvious that the thermodynamic temperature and the double-ratio temperatures are identical in this case. The dashed lines (V_{int}) refer to the temperatures calculated from Eq. (15) but with the inclusion of final state interaction (nuclear+Coulomb) over the barest scenario for the fragment generation. In all the cases investigated, it is found that the inclusion of fragment-fragment interaction ($\mathcal{V}$) shifts the temperature by nearly a constant amount at all excitations; the amount of shift or its sign depends on the particular isotope combination chosen. The shift is found to be negligible for double ratios (He-d), (Li-He) and (Be-He). The dot-dash lines (QS) in the figures refer to calculations done with further inclusion of quantum statistics. As comparison of the dashed and dot-dash curves shows, no appreciable quantum effects are evident except in the case of the temperature obtained from the double ratios (Li-d). In this particular case, it is further seen that the difference between the quantum and classical (Maxwell-Boltzmann) calculations widens with excitation energy or with temperature. It is normally expected that at low density and high temperature [12], quantum effects would not be discernible, to be more exact, as explained earlier it depends on whether the fugacity $\eta \ll 0$. It is seen that the densities of the fragment species or alternatively their fugacity η vary in a complex way with the temperature. When the temperatue is low, the density is extremely low and hence the value of η is relatively large and negative; with increase in temperature along with density the value of η increases initially and then again decreases for the complex fragments. However for nucleons η increases monotonically in the energy regime that we consider. This complex variation of η is reflected in the temperatures extracted from the double ratio of yields obtained with quantum statistics.

In order to take into account effects due to side-feeding, we next assume that the fragments are produced in particle-stable excited states so that the ground state population from the γ-decaying states have to be considered. Side-feeding from particle decay is thus ignored. Kolomiets *et al.* [13]

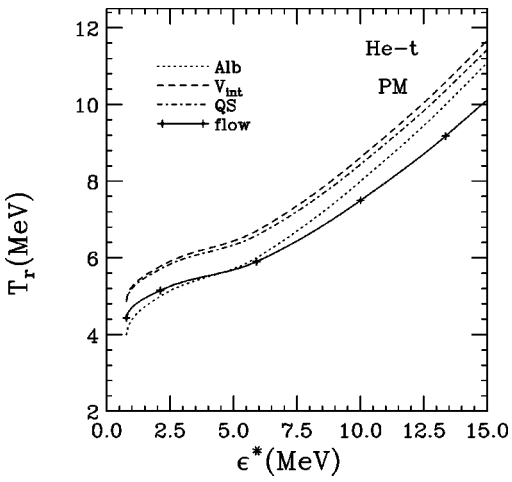

FIG. 3. Same as Fig. 2 for the $(^4\mathrm{He}/^3\mathrm{He})/(t/d)$ thermometer.

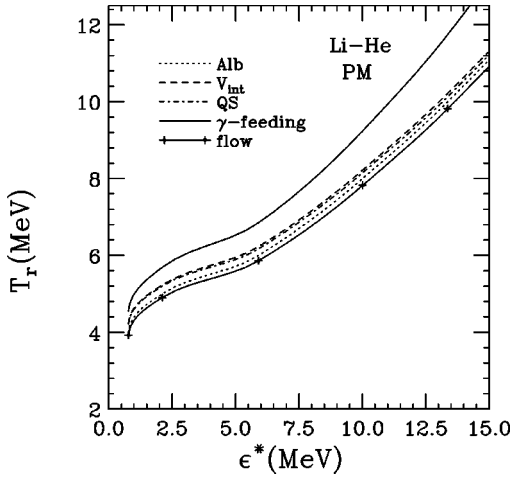

FIG. 5. Same as Fig. 4 for the $(^7\mathrm{Li}/^6\mathrm{Li})/(^4\mathrm{He}/^3\mathrm{He})$ thermometer.

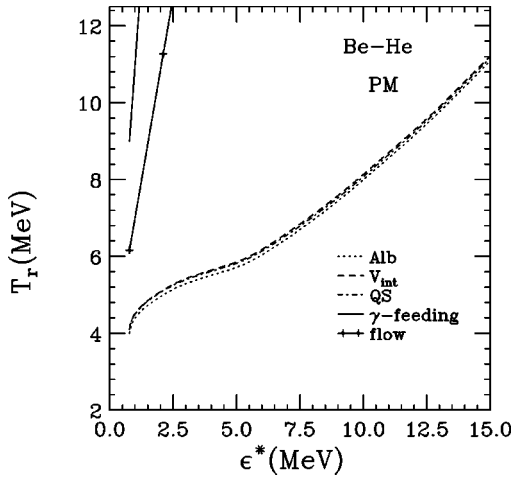

FIG. 6. Same as Fig. 4 for the (^{10}Be/^{9}Be)/(^{4}He/^{3}He) thermometer.

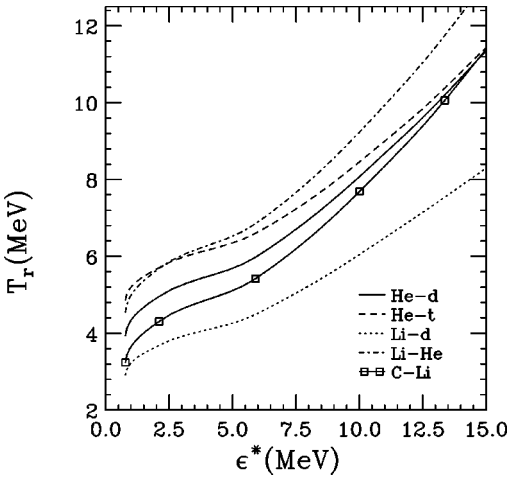

FIG. 8. The double-ratio temperatures T_r obtained after inclusion of final state interaction, quantum statistics and γ-feeding in the PM model. The fragmenting system is ^{150}Sm. The solid, dashed, dotted, dot-dash, and the full line with open squares refer to (He-*d*), (He-*t*), (Li-*d*), (Li-He), and (C-Li) thermometers, respectively.

have shown that particle-decay effects are rather negligible, further there is uncertainty about the cut-off limit to the particle decay width Γ that one should take which is intimately coupled with the time scale for prompt multifragmentation. Side-feeding effects are studied after generating the fragment yield by using Eqs. (6), (7), and (8) with flow pressure $P=0$. In these equations, ϕ is the internal partition function that includes a sum extending over the ground and γ-decaying excited states. For the fragments considered, isotopes up to ^{4}He were taken as billiard balls with no internal excitation as it has no low-lying γ-decaying state. Similarly for ^{9}Be, only the ground state was considered. For the rest, the excited states considered are 3.563 MeV for ^{6}Li, 0.478 MeV for ^{7}Li, 3.37, 5.958, 5.960, 6.018, and 6.26 MeV for ^{10}Be, 4.439 for ^{12}C and 3.089, 3.685, and 3.854 MeV for ^{13}C. For other heavier nuclei, continuum approximation is used for the single-particle levels and internal partition function is taken as $\phi=\int\rho(\epsilon)e^{-\epsilon/T}d\epsilon$ where the integration extends up to particle emission threshold. Over and above the quantum statistical effects, when we consider effects due to γ-feeding, it is found from Figs. 4–7 (by comparing the dot-dash and the full lines) that these effects are very sizable. The (He-*d*) and (He-*t*) thermometers show no side-feeding effects (Figs. 2 and 3) as these fragments are taken to have no excited states. A dramatic effect is seen for the (Be-He) thermometer (displayed in Fig. 6) where the sharply upward going full line refers to the temperature T_r obtained this way. Bondorf *et al.* [4] found a similar behavior for the Be-He thermometer.

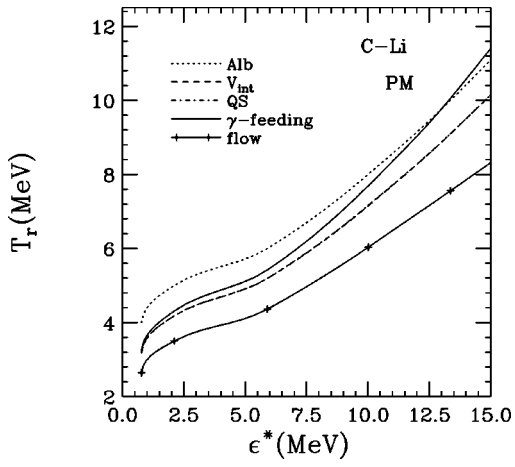

FIG. 7. Same as Fig. 4 for the (^{13}C/^{12}C)/(^{7}Li/^{6}Li) thermometer. The dashed and dot-dash curves cannot be distinguished from each other.

In central or near-central collisions between medium-heavy or heavy nuclei at intermediate or higher energies, compression and eventual decompression of the nuclear matter manifests itself in nuclear collective flow energy which might be a significant part of the total excitation. Collective flow influences the multifragmentation pattern to a significant extent [16,17]. The double-ratio isotope thermometer may then need to be recalibrated a great deal due to the nuclear flow. This is manifest from Figs. 2–7 where the full line with crosses correspond to calculated temperatures with inclusion of flow above the effects induced by fragment-fragment interaction, quantum statistics and wherever applicable, γ-feeding. The flow energy is taken to be 25% of the total excitation energy. Comparison of the full line with the line with crosses shows that at a given excitation energy, the temperature is always lower or for the same temperature, the excitation energy is always higher. In Fig. 8, all the double-ratio isotope thermometers except for Be-He are displayed for comparison. Except for the flow effects, other effects are included here. The behavior of the temperature profiles with excitation energy look nearly the same but their magnitudes differ depending on the choice of the thermometers. At lower excitations, an uncertainty in the $T_r\sim 2.0$ MeV involving (Li-*d*) and (Li-He) thermometers is found which increases progressively with excitation energy. The uncertainty involving (He-*t*), (He-*d*), and (C-Li) thermometers however decreases with excitation energy, all three temperatures converging at the highest excitation we study. In Fig. 9, the isotope temperature corresponding to (Li-He) is shown with inclusion of different magnitudes of flow. The full and dashed curves refer to cases when half (50%) and one fourth

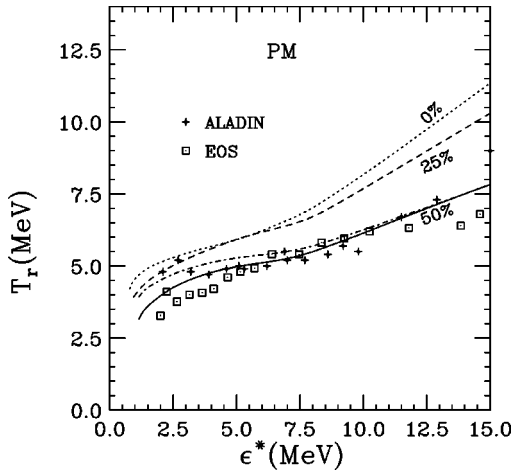

FIG. 9. The temperatures calculated with all effects as discussed in the text from the (Li-He) and (He-t) thermometers in the PM model. The fragmenting system is ^{150}Sm. The dotted, dashed and full lines refer to calculations for (Li-He) temperatures with 0%, 25%, and 50% of the total excitation as flow energy. The dot-dash line refers to the (He-t) temperatures with flow energy as 50% of the total excitation. The crosses refer to ALADIN data and the open squares refer to the data from EOS Collaboration.

(25%) of the total excitation have gone to the flow energy; the dotted curve corresponds to no flow. As an illustration, data from the ALADIN [5] and EOS [6] experiments are displayed in the figure, which use the (Li-He) and (He-t) thermometers respectively. To have a contact with the EOS data, we also display the calculated temperature from the (He-t) thermometer with 50% flow energy (dot-dash curve). In an analysis of the same data in Ref. [29], it was pointed out that the data could be better explained invoking progressive increase of the percentage of flow energy with increasing total excitation; comparison of the present calculations with the experimental data validates this observation.

B. Sequential binary decay

Hot nuclear systems may release energy through binary fissionlike decay, the decay chain continues till there is no further energy for binary division. At the end of such decay process, fragments of different species are produced in ground states and in γ-decaying excited states, the multiplicity depending on the initial system and excitation energy. It has been noted earlier [30] that the frequency distribution of the fragments follows almost a power-law distribution and that it is not too different from the one obtained from prompt multifragmentation at the same excitation energy. Our calculations done at different excitation energies also show that the inclusive mass or charge distrbutions obtained from both PM and SBD models are roughly the same. The isotopic distributions are however seen to have significant differences. In the SBD model, the hot nucleus prepared initially at an excitation energy or temperature goes through a succession of decays, the temperature of the produced fragments (assuming equilibration before each decay) therefore also decreases as time proceeds. In Fig. 10, we display the average temperature $T_{\rm av}$ of the produced fragments as a function of time when the initial system ^{150}Sm has been prepared at three different excitation energies, namely, $\epsilon^*=13.5$, 10.0, and 6.0 MeV. The temperature of the fragments is calculated from $T_{\rm av}=(10\langle\epsilon^*\rangle)^{1/2}$ where $\langle\epsilon^*\rangle$ is the ensemble averaged excitation energy per particle of the fragments at any particular instant of time. It is found that the higher the initial excitation energy of the system, the faster is the cooling rate which is expected. An experimentalist does not know *a priori* whether multifragmentation is a one-step process (PM) or is an outcome of a sequence of binary decays. If one takes the fragmentation yields from the SBD model as the ''experimental data,'' it would be interesting to see the results for the double ratio temperatures calculated with the Albergo prescription as given by Eq. (15). The double ratio temperatures so calculated for the combinations (He-d), (He-t), (Li-d), and (Li-He) are displayed in Fig. 11. One finds that except for (Li-d), the temperatures are very weakly dependent on the initial excitation energy and are very low ($\sim$3 MeV) even at the highest excitation energy we study. Such apparent temperatures were obtained by Ma *et al.* [31] in their Albergo-type analysis of the experimental data in ^{36}Ar+^{58}Ni collisions at 95A MeV. For the (Li-d) ther-

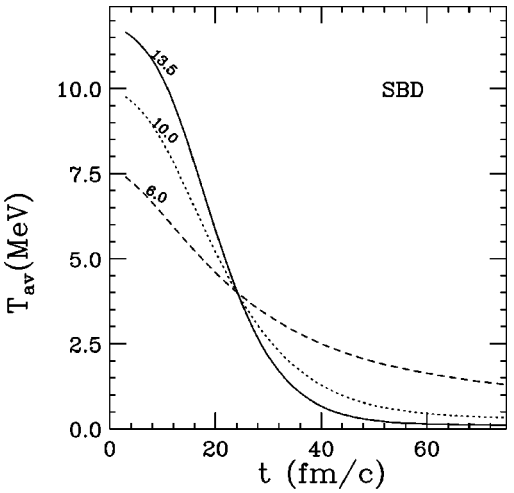

FIG. 10. Evolution of the average temperature $T_{\rm av}$ as a function of time for the ^{150}Sm nucleus prepared at excitations of 13.5, 10.0, and 6.0 MeV per nucleon respectively in the SBD model.

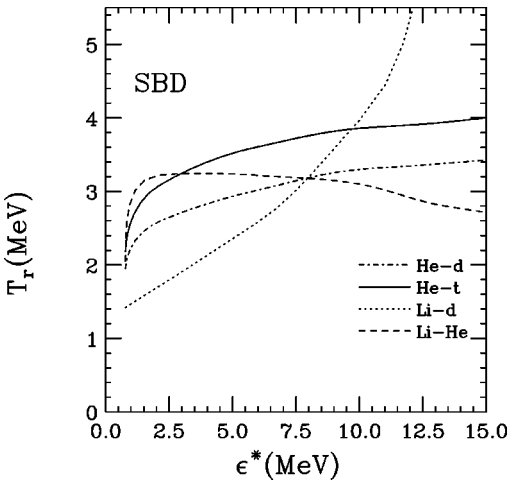

FIG. 11. The double-ratio temperatures from the thermometers (He-d), (He-t), (Li-d), and (Li-He) when the fragments have been produced in the SBD model from ^{150}Sm.

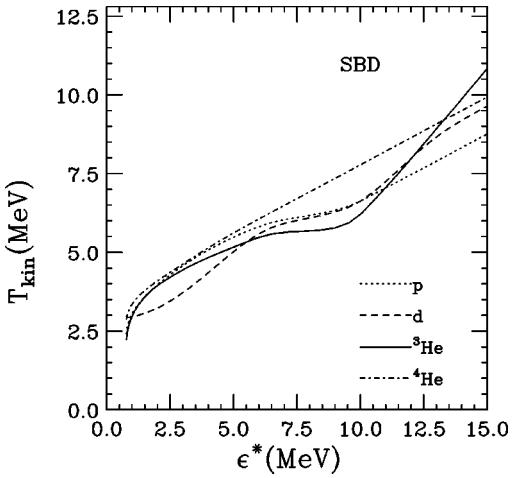

FIG. 12. The kinetic temperatures obtained from the energy distributions of the fragments p, d, ^{3}He, and ^{4}He produced in the disassembly of ^{150}Sm in the SBD model.

mometer, the temperature however rises steadily with initial excitation. Thus the functional dependence of the temperature T_r with excitation energy obtained from the SBD and PM models are very different; the thermometers in the SBD model also register too low a temperature compared to the PM model.

The kinetic energy distribution of the fragments at the end of the decay process would reflect the overall kinetic temperature of the system. In the SBD model, since the system proceeds through a sequence of temperatures, the kinetic energy distribution reflects an apparent temperature. In Fig. 12, this apparent temperature $T_{\rm kin}$ is shown as a function of initial excitation energy from the slope of the final energy distributions of p, d, ^{3}He, and ^{4}He produced from ^{150}Sm. The temperatures extracted from the four distributions are not very different. Closer inspection however shows that except for the one for ^{4}He, the ''caloric curves'' show broad plateaus mimicking a liquid-gas phase transition. This arises possibly from the changing temperature scenario and a complicated energy dependence of the fragment partial widths for decay in the SBD model.

IV. CONCLUSIONS

We have calculated the apparent temperatures from several combinations of the double ratio of isotope yields in two different physical scenarios in perspective; the one-step prompt multifragmentation and the sequential binary decay. In the PM model, the inclusion of final state interaction gives rise to nearly a constant shift in the temperature T_r calculated as a function of excitation energy from the one obtained from the Albergo prescription, the shift being different for different isotope combinations. The effect of quantum statistics on the apparent temperatures is found to be nominal; the effect of γ feeding is very substantial and is found to be rather dramatic for the (Be-He) thermometer. The presence of collective flow reduces the apparent temperature T_r for a given total excitation energy. Moreover, a soft plateau, generally seen in the caloric curves obtained for the double-ratio temperatures becomes extended with inclusion of flow energy. The import of our calculations is that better contact with the experimental data can be achieved if one assumes that the excitation energy has a collective flow component in it.

One cannot rule out the sequential binary decay as a possible reaction mechanism for the fragment yields, particularly at not too high excitation. This prompted us to study the caloric curves where the apparent temperatures T_r are calculated from the fragment yields in the SBD model, both from the double ratios and slopes of the energy distributions of the fragments. The double ratio temperatures generally show extended plateaux but no subsequent rise at higher excitations; on the other hand the caloric curves calculated from the slopes of the energy distributions display broad shoulders with subsequent rise at higher excitations mimicking a first-order phase transition. Since caloric curves obtained in both the PM model and the SBD model show apparent signatures of a phase transition, conclusion regarding phase transition in nuclear collision requires utmost caution and search for additional signatures is called for.

[1] W. A. Kupper, G. Wegmann, and E. R. Hilf, Ann. Phys. (N.Y.) **88**, 454 (1974).
[2] H. Jaqaman, A. Z. Mekjian, and L. Zamick, Phys. Rev. C **27**, 2782 (1983).
[3] D. Bandyopadhyay, C. Samanta, S. K. Samaddar, and J. N. De, Nucl. Phys. **A511**, 1 (1990) and further references therein.
[4] J. P. Bondorf, R. Donangelo, I. N. Mishustin, and H. Schulz, Nucl. Phys. **A444**, 460 (1985).
[5] J. Pochodzalla *et al.*, Phys. Rev. Lett. **75**, 1040 (1995).
[6] J. A. Hauger *et al.*, Phys. Rev. Lett. **77**, 235 (1996).
[7] J. B. Elliot *et al.*, Phys. Lett. B **418**, 34 (1998).
[8] S. Albergo, S. Costa, E. Costanzo, and A. Rubbino, Nuovo Cimento A **89**, 1 (1985).
[9] J. Randrup and S. E. Koonin, Nucl. Phys. **A356**, 223 (1981).
[10] F. Gulminelli and D. Durand, Nucl. Phys. **A615**, 117 (1997).
[11] P. R. Subramanian *et al.*, J. Phys. G **7**, L241 (1981).
[12] Z. Majka *et al.*, Phys. Rev. C **55**, 2991 (1997).
[13] A. Kolomiets *et al.*, Phys. Rev. C **54**, R472 (1996).
[14] J. P. Bondorf, A. S. Botvina, and I. N. Mishustin, Phys. Rev. C **58**, R27 (1998).
[15] M. J. Huang *et al.*, Phys. Rev. Lett. **78**, 1648 (1997).
[16] Subrata Pal, S. K. Samaddar, and J. N. De, Nucl. Phys. **A608**, 49 (1996).
[17] J. Desbois, R. Boisgard, C. Ngo, and J. Nemeth, Z. Phys. A **328**, 101 (1987).
[18] S. Shlomo, J. N. De, and A. Kolomiets, Phys. Rev. C **55**, R2155 (1997).
[19] W. J. Swiatecki, Aust. J. Phys. **36**, 641 (1983).
[20] Subrata Pal, S. K. Samaddar, and J. N. De, Nucl. Phys. **A591**, 791 (1995).
[21] Subrata Pal, S. K. Samaddar, J. N. De, and B. Djerroud, Phys. Rev. C **57**, 3246 (1998).
[22] S. K. Ma, *Statistical Mechanics* (World Scientific, Singapore, 1993).

[23] J. N. De, N. Rudra, Subrata Pal, and S. K. Samaddar, Phys. Rev. C **53**, 780 (1996).
[24] D. H. E. Gross, L. Satpathy, M. T. Chung, and M. Satpathy, Z. Phys. A **309**, 41 (1982).
[25] Subrata Pal, S. K. Samaddar, A. Das, and J. N. De, Nucl. Phys. **A586**, 466 (1995).
[26] R. K. Pathria, *Statistical Mechanics* (Pergamon Press, New York, 1985).
[27] A. Kolomiets, V. M. Kolomietz, and S. Shlomo, Phys. Rev. C **55**, 1376 (1997).
[28] J. N. De, S. Dasgupta, S. Shlomo, and S. K. Samaddar, Phys. Rev. C **55**, R1641 (1997).
[29] S. K. Samaddar, J. N. De, and S. Shlomo, Phys. Rev. Lett. **79**, 4962 (1997).
[30] J. A. Lopez and J. Randrup, Nucl. Phys. **A491**, 477 (1989).
[31] Y. G. Ma *et al.*, Phys. Lett. B **390**, 41 (1997).